SLAC-PUB-6376
October 1993
(I)

CsI ELECTROMAGNETIC CALORIMETER DEVELOPMENT FOR A LOW OR MEDIUM ENERGY e^+e^- COLLIDER

Mary E. King
Stanford Linear Accelerator Center
Stanford University, Stanford, California, USA

Abstract

Design considerations for an electromagnetic CsI calorimeter suitable for use at low and medium energy, high-luminosity e^+e^- storage rings are presented, together with results of a test of an array of CsI(Tl) crystals in an e^- / π^- beam (120 to 400 MeV) at TRIUMF. The crystal array used in the test was designed to explore longitudinal and transverse crystal segmentation, and a redundant wavelength-shifter and photodiode readout system. Energy resolution of $(1.69 \pm 0.08)\%/\sqrt{E}$ and $(1.83 \pm 0.05)\%/\sqrt{E}$ was obtained for two different crystal tower configurations. Position resolution of 6.5 (9.0) mm was obtained at 300 (120) MeV for four 4 x 4 cm^2, 4 rl. CsI crystals.

Presented at the Third Workshop on the Tau-Charm Factory, Marbella, Spain, June 1-6, 1993

* Work supported in part by the U.S. Department of Energy Contract DE-AC03-76SF00515.

1. INTRODUCTION

Several high-luminosity, low and medium energy e^+e^- storage rings are under consideration for future construction. Each of these facilities will feature a state-of-the-art detector with high precision electromagnetic calorimetry. Numerous studies [1] of requirements for these detectors suggest that many characteristics of CsI crystal calorimetry are necessary to achieve their physics goals. Specifically, the high light yield (~50,000 photons/MeV) of CsI(Tl) or CsI(Na) facilitates excellent energy resolution, and efficient detection of photons with energies down to a few MeV. Excellent position and angular resolution is also attainable at these energies. The large light output of CsI crystals makes feasible the use of low-gain or unity-gain devices, such as photodiodes, for readout. The dominant drawbacks of CsI scintillators are poor mechanical properties, low radiation hardness, and relatively long decay times (~1 μsec for Tl-doped CsI crystals) which integrate scintillation light over many beam crossings. While radiation hardness is not an issue at Φ and Tau-Charm Factories [2], evidence from experiments with large CsI arrays suggests that albedo and pileup may limit the use of the lowest energy photons ($\leq$ 20 MeV) if these backgrounds are not adequately suppressed. The long decay time may result in serious sources of low-energy "fake" photons from the pileup of lost beam particles, nuclear interactions of hadrons, and albedo within an event. These crystals should not be considered for such future colliders unless these issues are resolved [3].

2. CALORIMETER AND TEST DESIGN

We [4] tested an array of CsI(Tl) crystals which could be scaled to a full-sized cylindrical detector suitable for low and medium energy "factories". Physics and cost considerations imply that a "factory" detector would typically contain about 8-10 m^3 of crystals in a cylindrical volume ~3.5 meters long and of ~1 meter inner radius. It would be further segmented into ~10,000 projective towers. The towers would be of transverse size (40-80 mr) x (40-80 mr), and 16-18 rl. (29.8-33.5 cm) long, tapered along their major axis to form truncated pyramids. To enhance $\pi / \mu / e$ separation and improve the rejection of fake photons, towers can also be segmented longitudinally into two parts. Depending on the average energy in the collisions, a break around shower maximum, at ~3 to 4 rl. (5.6-7.4 cm), would be chosen.

The electronics for a CsI calorimeter has strict limits on inherent noise. Because of this, it is desirable to locate close to the crystals most of the signal processing, such as amplification, pulse shaping, calibration, and drivers. Since these electronics would be inaccessible during an experimental run, a high degree of reliability is desirable. Other design considerations are spatial constraints and heat dissipation. To allow energy to be unambiguously associated with a beam

crossing, we also anticipate a need to incorporate coarse timing information into the analog readout of a final device.

2.1 TRIUMF Beamline and Instrumentation

Our test of a longitudinally-segmented CsI(Tl) array was conducted in the TRIUMF M11 and M13 beamlines. Only results from data taken in the TRIUMF M11 beamline are presented here. A schematic of the beam line is shown in Fig 1. Readout of data was triggered by a coincidence of RF timing with signals in two 3mm thick scintillators. To avoid pileup, upstream collimators were used to reduce the rate of incident particles to ~100 Hz. Signals from the scintillator S1 and RF were used to measure time-of-flight (TOF), which provided modest π / μ separation up to ~400 MeV. A low-mass, eight-wire drift chamber was used to measure the position and angle of the beam at the crystal face. Thirteen crystal towers were stacked in configuration in an aluminum box through which dry N_2 flowed. The dry box contained a thin aluminum foil beam entrance window.

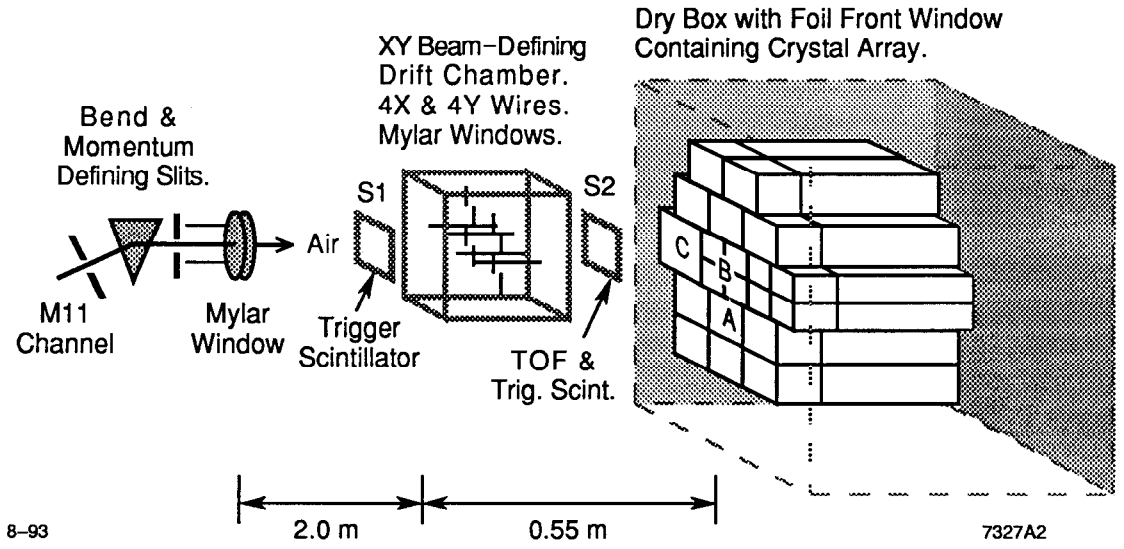

Fig. 1. The TRIUMF M11 beamline with trigger scintillators S1 and S2, beam-defining hodoscope, and CsI crystal array in dry box. The locations of Towers A, B, and C discussed in this text are indicated by the labels of A, B, and C, respectively.

2.2 Geometry of Crystal Array

Three lateral geometries were considered: crystals of rectangular cross section with faces of 6.4 x 6.4 cm^2, front and back, and an 8.0 x 8.0 cm^2 face in the back either subdivided four-fold in the front, or not, as shown in Fig. 2. The beam test array consisted of 12 6.4 x 6.4 cm^2 and three 8.0 x 8.0 cm^2 crystals. Each crystal within a tower was optically separated from the other crystals with a wrapping of three layers of PTE Teflon and one layer of aluminized mylar (total thickness ~ 0.13 mm). After wrapping, each crystal was "tuned" with a Cs^{137} source such that the variation in light output along each crystal's major axis on all four sides was $\leq 2\%$.

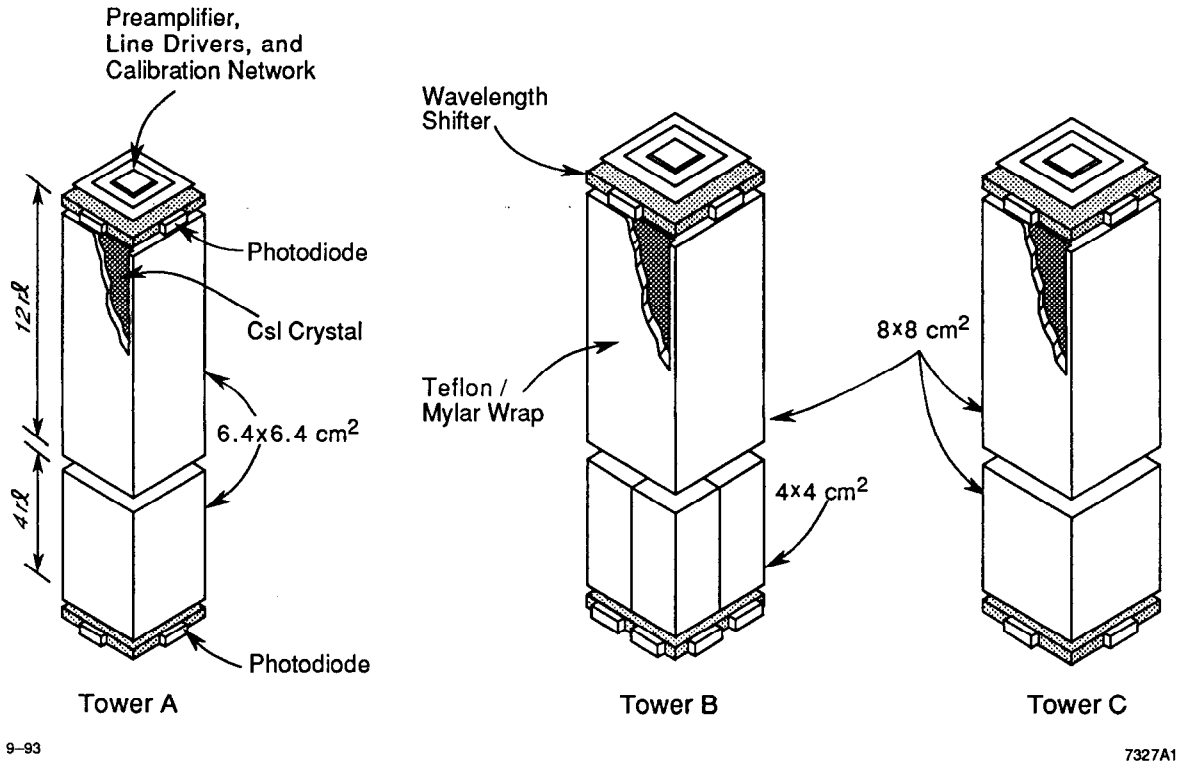

Fig. 2. Schematic of the three configurations of CsI calorimeter crystal towers tested, showing longitudinal and transverse segmentation of crystals, and wavelength shifter-photodiode-preamplifier readout. Configurations labeled Towers A, B, and C, respectively, correspond to the configuration of each of those particular towers analyzed herein.

2.3 Wavelength Shifter and Photodiode Construction

The light collection for the readout of each crystal was accomplished using a 3 mm-thick wavelength-shifting acrylic plastic (WLS) that covered about 70% of one face of the crystal. The WLS acted as a light guide to bring wavelength-shifted light to a photodiode placed on its narrow edge. One WLS covered the front face of the front crystal and one WLS covered the back face of the back crystal. The other sides of each crystal were wrapped with materials described in the previous section, as illustrated in Fig. 2. Hamamatsu S3588-01 photodiodes (PD's), each with an active area of 3.4 x 0.3 cm^2, were affixed to the WLS edges with Summers Laboratories Lens Bond F-65 adhesive. Four photodiodes were placed on each WLS (one/edge), except for the WLS's associated with the 4 x 4 cm^2 crystals, where spatial constraints permitted the use of only two PD's/WLS. White reflective paint coated the balance of the WLS edges, and white reflective paper was loosely placed on the surface opposite to that of the crystal face.

We used four PD's/WLS to provide redundancy and to improve the signal-to-noise ratio. The addition of a photodiode to a WLS edge, rather than covering a WLS edge completely with white reflective paint, results in additional net light collection equal to about 95% of the possible total light output of the crystal into a single PD. Four PD's, one on each edge of the WLS, increase the signal by about 3.2, while the electronic noise increases by only a factor of two if each PD is individually amplified, for a net gain of 1.6 in signal-to-noise.

2.4 Overview of Readout Electronics

While it may be desirable to put several preamplifiers on one circuit board for a "factory" CsI calorimeter, in the beam test, for each PD, there was a separate preamplifier board. The circuitry on each preamplifier board consisted of a FET and ASIC-based charge amplifier, a calibration network, and differential line drivers. Bias voltage for the PD, power, and calibration signals were also routed on the board. To reduce pickup, all PD signals were carried to the preamplifiers on 0.3 mm-diameter micro-coaxial cable of 1.5 pf/cm capacitance. The cables were placed along the inner edges of the G-10 boxes containing the crystals and behind them was placed one preamplifier board for each photodiode in the crystal tower.

Differential signals passed out of the dry box on 5 m-long ribbon cables. They were received single-ended by CLEO-II-style shaping amplifiers which performed a single integration with shaping and peaking times of 3 μsec. Shaped signals were sampled with a ~200 ns gate around the peak, and digitized by LRS 2289A ADC's. There was a total of 132 readout channels. The preamplifier and shaping amplifier gains were separately preadjusted to give equal signals

for a fixed charge injected at the inputs. Each calibration circuit was trimmed to produce a constant charge for a fixed calibration pulse input. The final electronic calibration employed a sequence of 100 DAC-set pulses, at 15 distinct values, readout through the ADC's. To remove a small nonlinearity at the low end of the ADC range, the calibration data was fit with two quadratic functions.

3. TEST RESULTS

Results are presented for three crystal towers, each having a different geometrical configuration. As shown in Figs. 1-2, Tower A refers to a contained 6.4 x 6.4 cm^2 crystal tower, Tower B refers to a contained 4 x 4 cm^2 crystal tower, and Tower C refers to an uncontained 8 x 8 cm^2 crystal tower. A contained tower is one that is surrounded on all sides by other towers, so that energy shared with adjoining towers can be taken into account in determining resolutions. To determine the energy resolution and test linearity, we evaluated data taken at three beam energies, for each of the three tower configurations (120, 250, and 400 MeV for Towers A and B, and 120, 200, and 400 MeV for Tower C). Position resolution was studied for Towers B and C at four beam energies (120, 200, 250 and 300 MeV).

3.1 Calibrations

Once an electronic calibration has been performed, the single monolithic crystals which have been used in the CLEO-II and Crystal Barrel detectors require a single overall gain constant to relate light output to energy. In contrast, the longitudinal segmentation of crystals within a tower introduces an additional calibration constant for each tower, so the beam test data was calibrated to the beam energy in two steps. One beam energy was chosen to perform the calibration for each tower. First, the gain constant of each PD signal was adjusted so that all diodes on a single crystal (either front or rear) read the same average signal at the beam calibration momentum. Since the beam contained both e^-'s and π^-'s, this calibration can be done using either the distinct peaks of the minimum-ionizing-particle or the averages of the showering-particle spectra.

The additional calibration involves the relative weighting of signals from PD's associated with the front and back crystals in the tower. To find the front-to-back (F/B) weighting constant, signals from all PD's on each crystal in a tower were summed and the average taken. The average signals from the front and back crystals in the tower were scaled such that their intercepts were equal to the beam energy. The correct F/B ratio produces a minima for the energy

resolution. For all towers, calibrations were performed at the highest beam energy for which data was available ($\leq$ 400 MeV).

3.2 Linearity of Response and Energy Resolution

To determine energy resolution and linearity, a time-of-flight cut was made to select e^-'s, and minimum energy cuts were made to reject minimum ionizing particles. Additionally, to guarantee a single well-defined trajectory, using the beam-defining drift chamber hodoscope, a track quality cut was made, requiring at least two hits in one dimension and at least three hits in the other dimension. A fiducial cut limiting the beam profile to 3 x 3 cm^2 was then imposed.

After applying these criteria, to determine the energy resolution for beam incident in a given tower, the energy collected in the eight adjoining towers was added to the energy for that tower. This observed energy was then rescaled at the calibration beam energy. The distributions of total energy deposited at different beam energies were then fit with a Gaussian to determine the peak and the width, or σ_E/E. To avoid low energy radiative tails, the spectra were fit from 50 to 95% of their central value. Systematic errors resulting from the fit were estimated by varying the endpoints and background shapes in the fit on each side of the central value.

The linearity of each tower was determined by calibrating at one beam energy, then measuring the central value of the spectra at the other beam energy. The linearity is sensitive to the F/B weighting, and to the lateral sharing of energy. Using this calibration procedure, as indicated by the result in Table 1, we observe a linearity of better than 1%.

Results for Towers A and B at three beam energies are summarized in Table 1 and illustrated in Figs. 3a and 3b. The result of a fit to the energy resolution versus incident momentum for Tower A is:

$$\frac{\sigma_E}{E} = \frac{0.0183 \pm 0.0005}{\sqrt{E}},$$

and for Tower B is:

$$\frac{\sigma_E}{E} = \frac{0.0169 \pm 0.0008}{\sqrt{E}}.$$

Table 1. Results for contained crystal tower arrays A and B.
Asterisk (*) indicates calibration energy.

Tower Size (cm^2)	Beam Energy (MeV)	Measured Energy (MeV)	σ_E (MeV)	Energy Resolution (σ_E / E)
TOWER A	120	124.1 ± 0.5 ±0.5	6.6 ± 0.3±0.3	0.053 ±0.003 ± 0.003
6.4 x 6.4	250	252.1 ± 0.5 ±0.6	9.4 ± 0.3±0.4	0.037 ±0.001 ± 0.002
	400*	400.0 ± 1.1 ± 0.9	9.7 ± 1.1±0.3	0.025 ±0.003 ± 0.008
TOWER B	120	130.5 ± 0.4 ± 0.4	6.7 ± 0.3± 0.3	0.052 ±0.003 ± 0.002
4-4 x 4	250	252.7 ±0.8 ±0.4	8.2 ± 0.6±0.3	0.033 ±0.002 ± 0.001
	400*	400.0 ± 1.2 ± 0.7	10.2 ± 0.5±0.8	0.026 ±0.002 ± 0.001

Energy resolution results for Tower C, which was uncontained, a comparison of energy resolution data with Monte Carlo simulation, and a more extensive discussion of electronics, are presented elsewhere [5].

4. POSITION RESOLUTION

Crystals with transverse dimensions comparable to their Moliere radius (~3.8 cm for CsI(Tl)) can take advantage of the spreading of a shower into neighboring crystals to accurately measure position. A position calculation using a simple center-of-gravity method consists in taking the energy-weighted average of the central and neighboring crystals' positions using the formula:

$$CG = \sum_i \frac{E_i \bullet x_i}{E_i},$$

where x_i is the center of crystal i, and E_i is the energy deposited in crystal i. For showers contained largely within the central crystal tower, this expression is dominated by the position of the incident tower, and varies little with incident beam position until near the edges of the crystal,

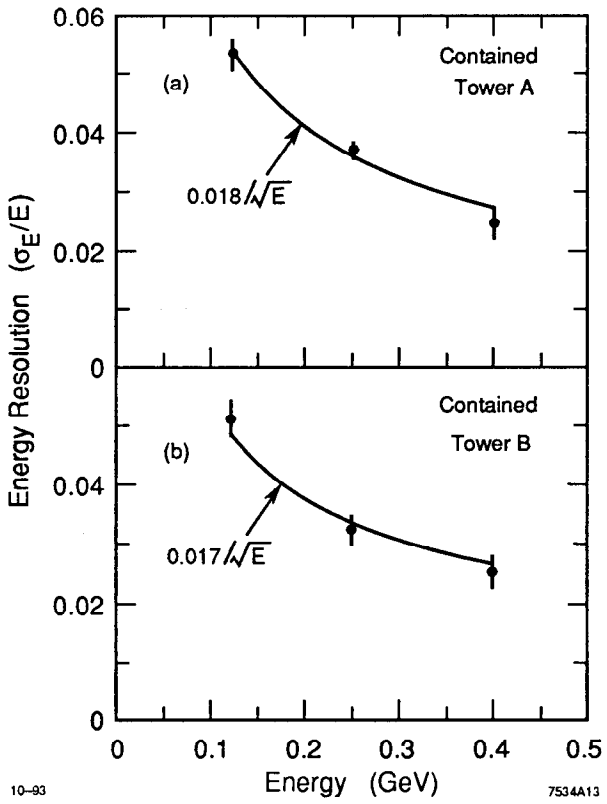

Fig. 3. Energy resolution results, with lines indicating fits to the data, for Towers A & B.

where shower sharing starts to become important. Instead of employing this basic center-of-gravity method, we have used a corrected-center-of-gravity technique to determine the position resolution. The corrected center-of-gravity position is calculated by finding the average true position, given by the beam-defining hodoscope, as a function of the center-of-gravity value. This corrected center of gravity is then used to determine the resolution by taking, for each event, the difference between itself and the true position, as defined by the hodoscope. This method for determining position resolution is based on a mathematically equivalent technique used by CLEO [6]. The resolution histograms were then fit with a Gaussian function to obtain the quoted resolutions.

Position resolutions were calculated for Towers B and C. Resolution was determined using e^-'s, with the same time-of-flight and energy deposition cuts as was used for energy resolution studies. Position resolution for Tower C was calculated using the energy deposited in the front and back crystals in the tower. Since Tower C was illuminated on only one side, it was necessary to fold the resolution plot across the center. This introduces a systematic error the size of which can be estimated by studying the effects of the same folding on Tower B. The position

resolution for Tower B was determined using the four-4 rl thick front crystals only, taking advantage of their smaller lateral dimensions.

The average resolution was determined from a subset of all tracks in a given crystal tower. The tracks were chosen to enforce a uniform illumination across the tower's face. The average position resolution results are summarized in Table 2. As a function of energy, the position resolution can be parameterized in the form:

$$\sigma_X = a + \frac{b}{\sqrt{E}},$$

where the values for a and b for Towers B and C are given in Table 3. Fits of the position resolution results to this form are shown in Fig. 4.

Table 2. Position resolution results for Towers B and C. Statistical errors are given for both towers. The systematic (second) error on the resolution for Tower C takes into account the fact that only half of the tower was illuminated.

Beam Energy (MeV)	**Tower B, 4 x 4 cm^2 front crystals only Resolution (mm)**	**Tower C, front and back crystals Resolution (mm)**
120	9.1 ± 0.1	$15.1 \pm 0.1 \pm 0.7$
200	8.0 ± 0.1	$11.8 \pm 0.1 \pm 0.4$
250	7.0 ± 0.1	$11.9 \pm 0.1 \pm 0.4$
300	6.5 ± 0.2	$11.9 \pm 0.2 \pm 0.6$

Table 3. Position resolution results for Towers B and C for the fit $\sigma_X = a + \frac{b}{\sqrt{E}}$.

Crystal Tower	**a (mm)**	**b (mm-GeV$^{0.5}$)**
Tower B, 4 x 4 cm^2 front crystals only	2.5 ± 0.9	2.3 ± 0.4
Tower C, front and back crystals	5.8 ± 2.8	3.0 ± 1.5

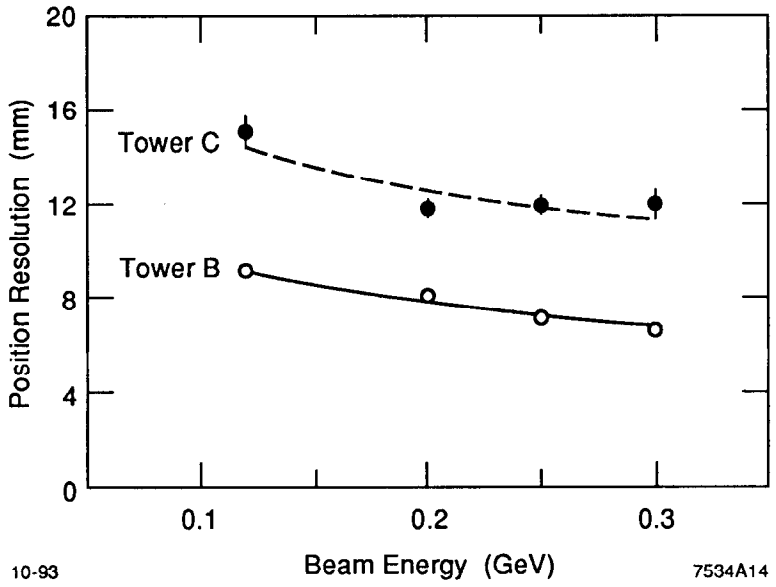

Fig. 4. Position resolution for the front 4 x 4 cm^2 crystals in Tower B and for the front and back crystals in Tower C, each fit with the form a + b/$\sqrt{E}$, where a and b are given in Table 3.

5. CONCLUSION

We have presented results on energy resolution and linearity, and position resolution, for specific crystal tower configurations in an array of longitudinally-segmented CsI(Tl) crystals, where each crystal is readout with a wavelength shifter and two to four photodiodes. These measurements demonstrate that linearity and energy resolution are preserved in the presence of a longitudinal division of the crystals, near shower maximum. The longitudinal division of crystals within the towers can provide additional information on particle identification, range, and direction. This additional information may be necessary for background rejection in high luminosity e^+e^- and hadron colliders.

For contained towers, when energy shared with adjoining towers is taken into account, the energy resolution achieved appears independent of the type of tower configuration. We find an energy resolution consistent with (1.83 $\pm$ 0.05)%/$\sqrt{E}$ for Tower A and (1.69 $\pm$ 0.08)% for Tower B. The position resolution improves slowly with finer crystal segmentation and can be parameterized as a + b/$\sqrt{E}$, where for Tower B, (a,b) = ((2.5 $\pm$ 0.9) mm, (2.3 $\pm$ 0.4) mm-$GeV^{0.5}$) and for Tower C, (a,b) = ((5.8 $\pm$ 2.8) mm, (3.0 $\pm$ 1.5) mm-$GeV^{0.5}$).

ACKNOWLEDGMENTS

I would like to acknowledge all those [4] who participated in the CsI array beam test at TRIUMF and in the analysis of the data collected there. For their gracious assistance during our beam test, we are grateful to the TRIUMF physicists and staff, particularly D. Ottewell and D. Diel.

REFERENCES

[1] See for example, R. H. Schindler, *Proceedings of the Tau-Charm Factory Workshop,* SLAC, Ed. L. Beers, SLAC REPORT-343 (1989) 127.

[2] D. Stoker, *Proceedings of the Tau-Charm Factory Workshop,* Universidad de Sevilla, Andalucia, Spain (May 1991).

[3] R. Schindler, in *Proceedings of the Tau-Charm Factory Workshop,* Universidad de Sevilla, Andalucia, Spain (May 1991).

[4] Beam test participants were R. Baggs, D. Coward, R. Coxe, D. Freytag, M. E. King, G. Niemi, G. Putallaz, R. H. Schindler, D. Stoker,‡ and E. Vokurka of Stanford Linear Accelerator Center, Stanford, CA; A. Foland and G. Gladding of University of Illinois, Champaign-Urbana, IL; K. Curtis, J. Dyke, and R. Johnson of University of Cincinnati, OH; E. Church, V. Cook, F. Toevs, and E. Weiss of University of Washington, Seattle,WA; R. Frey of University of Oregon, Eugene, OR; J. Izen and R. S. Davis of University of Texas, Dallas, TX, and W. Lockman of University of California, Santa Cruz, CA. ‡ Now at *University of California, Irvine CA 92717.*

[5] SLAC-PUB-6319, to be submitted to Nuclear Instruments & Methods.

[6] E. Blucher, *et al.*, Test of Cesium Ioidide Crystals for an Electromagnetic Calorimeter. NIM A 249, 201 (1986).